Reversible Helix−Helix Transition of Poly(*β*-phenylpropyl L-aspartate) Involving a Screw-Sense Inversion in the Solid State

Junji Watanabe,* Satoshi Okamoto, Koji Satoh, Koichi Sakajiri, and Hidemine Furuya

Department of Polymer Chemistry, Tokyo Institute of Technology, Ookayama, Meguro-ku, Tokyo 152, Japan

Akihiro Abe

Department of Industrial Chemistry, Tokyo Institute of Polytechnics, 1583 Iiyama, Atsugi-shi 243-02, Japan

Received April 22, 1996; Revised Manuscript Received August 12, 1996[⊗]

ABSTRACT: Poly(*β*-phenylpropyl L-aspartate) exhibits a novel helix−helix transition in the solid state at around 160 °C. The transition takes place reversibly in a narrow temperature range during a heating and cooling cycle, indicating that it is essentially of a first order. A combined use of circular dichroism, X-ray, and ^{13}C CP/MAS NMR measurements revealed that the transition is due to an interconversion of the helical screw sense from a right-handed α-helix to a left-handed helix. An unwinding and rewinding of the helical screw occurs concertedly along the polypeptide backbone without disturbing the uniaxial orientation of the helix axes.

1. Introduction

It is known that poly(L-aspartic acid ester)s form an α-helix in either the right-handed or left-handed screw-sense depending on the chemical structure of the side group (R), temperature, and solvents.[1−5] While poly(*β*-

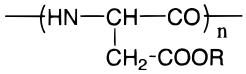

benzyl L-aspartate) (PBLA) and poly(*β*-methyl L-aspartate) adopt a left-handed α-helix in chloroform, right-handed forms are more popular among poly(L-aspartic acid ester)s having longer alkyl side groups such as R = CH_2CH_3 or $(CH_2)_2Ph$ (Table 1). In our previous studies on poly(*β*-phenethyl L-aspartate) (PPLA), we found that the transition between the two α-helical forms takes place reversibly in solution as a function of temperature.[6−9] The transition was observed in the dilute isotropic solution as well as in the anisotropic liquid-crystalline solution within a certain temperature range (80−100 °C). The ^2H NMR studies on PPLA in the lyotropic liquid-crystalline solution suggest that the uniaxial orientation of the backbone is maintained during the screw-sense inversion of the α-helix. In order to elucidate the mechanism of the transition, the spatial configuration of the side chain flanking the PPLA backbone has been extensively studied.[8−10]

PPLA is known to exhibit a screw-sense inversion from the right-handed α-helix to the left-handed *π*-helix in the solid state at about 130 °C.[11] PBLA and its derivatives carrying a methyl or chloro substituent at the para position of the terminal aromatic residue are known to exhibit a screw-sense inversion from the right-handed α-helix to the left-handed *ω*-helix at around 150 °C.[12−14] Recently, one of the present authors has reported a helix−helix transformation of poly(L-aspartic acid ester) with long *n*-alkyl side chains (R = $(CH_2)_nH$, $n = 12-18$) at around 150 °C.[15] In all these examples, however, the transition is observed only on heating and the high-temperature form remains unchanged on cooling.

Table 1. Experimentally Observed Helix Sense of Poly(L-aspartic acid ester)s in Solution

R	solvent	helix sense	ref
$-(CH_2)_xH$			
$x = 1$	chloroform	left (30 °C)	3, 5
$x = 2$	chloroform	right (30 °C)	5
$x = 3$	chloroform	right (30 °C)	5
		left (60 °C)	5
$-(CH_2)_xPh$			
$x = 1$ (PBLA)	chloroform	left (30 °C)	1, 2
$x = 2$ (PPLA)	chloroform	right (30 °C)	3, 5
	tetrachloroethane	right (30 °C)	6, 7, 8
		left (100 °C)	6, 7, 8
$x = 3$ (PPPLA)	tetrachloroethane	right (30 °C)	this work
		left (100 °C)	this work

In this work, we have extended our study to include poly(*β*-phenylpropyl L-aspartate) (PPPLA) with R = $(CH_2)_3Ph$. The most significant result obtained here is that the transition takes place reversibly between the right-handed α-helix and the left-handed helix in the solid state as well as in the dilute solution.

2. Experimental Section

2.1. Materials. PPPLA was prepared by a standard NCA method. *N*-Carboxy *β*-phenylpropyl L-aspartate anhydride was synthesized from triphosgene and *β*-phenylpropyl L-aspartate according to Daly's prescription.[16] A well-purified NCA was polymerized in 1% (w/v) chloroform by using triethylamine as an initiator for about 5 days. The molecular weight of the PPPLA sample thus obtained was estimated to be 66 000 from viscosity measurements in a mixture of dichloroacetic acid and chloroform at 25 °C.[17] A solid film was prepared by casting from a chloroform solution.

2.2. Measurements. The differential scanning calorimetry (DSC) was carried out with a Perkin-Elmer DSC Model II at a scanning rate of 10 °C/min. The circular dichroism (CD) and optical rotatory dispersion (ORD) were studied with a Jasco J-20 spectrometer. X-ray measurements were carried out by using a Rigaku-Denki X-ray generator with Ni-filtered Cu Kα

* To whom correspondence should be addressed.

[⊗] Abstract published in *Advance ACS Abstracts,* September 15, 1996.

S0024-9297(96)00596-7 CCC: $12.00

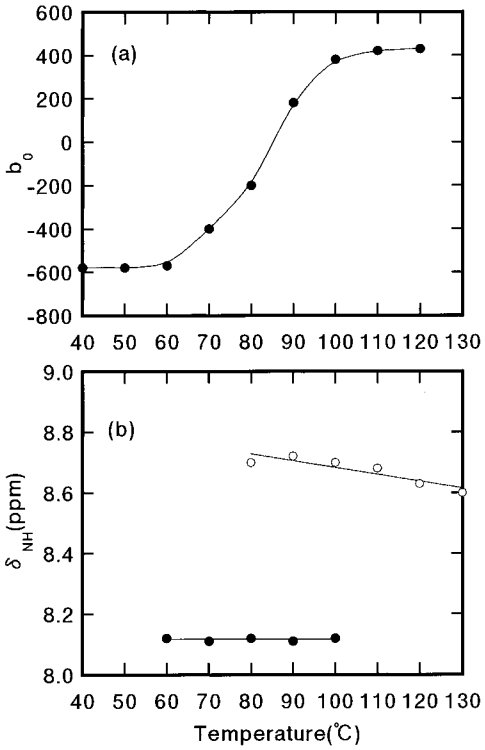

Figure 1. Variation of (a) Moffit−Yang b_0 and (b) ^{1}H chemical shift of the amide hydrogen δ_{NH} as a function of temperature, observed in TCE (1% v/v) ((■) right handed; (□) left handed).

radiation, equipped with a flat imaging plate (R-AXIS IID). An oriented film was prepared for the X-ray analysis by shearing unidirectionally a liquid-crystalline chloroform solution cast on a glass plate. Reflection spacings were calibrated by using a silicon standard. The temperatures of the sample holder were regulated within ±1 °C by using a Mettler FP 82 hot stage; in this heating system, only the reflections with spacings greater than 3.5 Å are observable because of the limited size of the window. The ^{1}H NMR spectra were recorded on a JEOL GSX-500 spectrometer operating at 500 MHz. The ^{13}C cross-polarization/magic angle spinning (CP/MAS) NMR spectra were measured by means of a JEOL GSX 270 NMR (67.5 MHz) with a variable-temperature (VT) accessory. The sample (ca. 200 mg) was charged in a cylindrical rotor made of ceramics and spun at 3−4 kHz. The contact time was 2 ms and the repetition time was 5 s. The spectral width and the number of data points were 27 kHz and 8K, respectively. The ^{1}H field strength was 1.6 mT for both the CP and decoupling processes. The number of accumulations was 200−400 to achieve a reasonable signal to noise ratio. The ^{13}C NMR chemical shifts were calibrated indirectly through external adamantane (29.5 ppm relative to TMS). Spinning sidebands due to an insufficient spinning rate were removed by a total suppression of the sidebands (TOSS) method.[18] Calibration of the temperature of the NMR probe was carried out by using a thermolabel sheet.

3. Results

3.1. Helix−Helix Transition in Dilute Solution. The ORD and ^{1}H NMR measurements were carried out for a dilute tetrachloroethane (TCE) solution (1% v/v) over a temperature range 40−130 °C. The results are illustrated in Figure 1, where the b_0 value obtained from the Moffit−Yang plot (Figure 1a) and the chemical shifts (δ_{NH}) characteristic of the right-handed and left-handed α-helices (Figure 1b) are plotted against temperature. Variation of the b_0 value indicates that the right-handed α-helix transforms into the left-handed form at higher temperatures. Chemical shifts of the amide hydrogen are appreciably different between these two α-helical

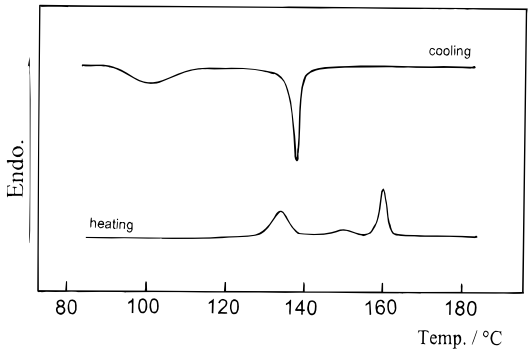

Figure 2. DSC thermograms of a PPPLA film measured at a scanning rate of 10 °C/min.

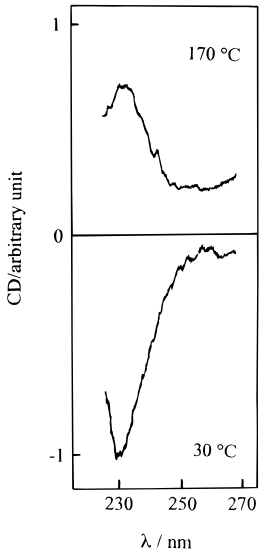

Figure 3. CD spectra of a PPPLA film at (a) room temperature and (b) 170 °C.

forms. The transition is therefore unambiguously demonstrated in the δ_{NH} vs temperature plot. The transition takes place between 80 and 100 °C in the dilute TCE solution.

3.2. Helix−Helix Transition in the Solid State. DSC thermograms obtained from a PPPLA film are shown in Figure 2. Three endothermic peaks were observed at 135 (T_1), 149 (T_2), and 159 °C (T_3) on heating and two exothermic peaks at 138 and 100 °C on cooling. The transitions were thermally reversible; the T_2 and T_3 transitions observed during the heating process merged into a single peak (138 °C) on cooling. The enthalpy changes (ΔH) estimated from the heating trace are 0.31, 0.07, and 0.37 kcal mol^{-1} per repeat unit for the T_1, T_2, and T_3 transitions, respectively.

Figure 3 shows the CD absorption spectra for the n−π^* transition around 230 nm: one taken at room temperature and the other at 170 °C, well above the T_3 transition (159 °C). The profiles of the two spectra are similar, but the sign is opposite: negative at room temperature, but positive at 170 °C. These observations indicate that the helix transforms from the right-handed to the left-handed regime as temperature increases. Shown in Figure 4 is the variation of the intensity of the CD spectra (at 230 nm) with temperature. No significant changes are observed in the intensity at the T_1 and T_2 transitions. As manifestly shown by the sign inversion, the helix-sense transformation takes place reversibly at the T_3 transition.

Figure 5a shows the X-ray pattern of an oriented film taken at room temperature from the edge-view position

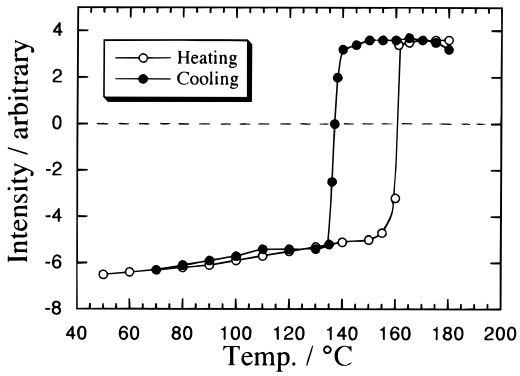

Figure 4. Temperature dependence of the intensity of the CD spectrum at 230 nm. The open and closed circles were collected on heating and cooling, respectively.

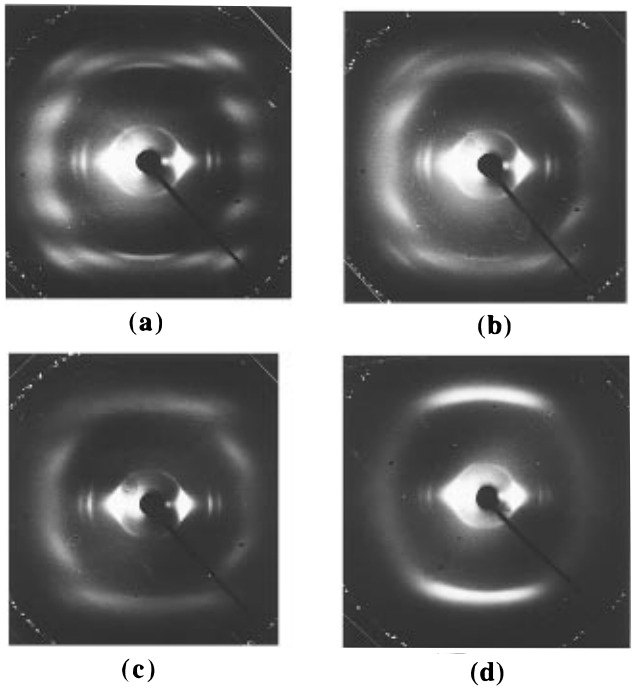

Figure 5. X-ray photographs of an oriented PPPLA film observed at (a) 30, (b) 140, (c) 150, and (d) 160 °C.

with a beam parallel to the film surface. The three equatorial reflections were observed and indexed with a two-dimensional hexagonal lattice of $a' = 15.6$ Å (see Table 2). The layer reflections are somewhat broad except for the strong reflection at 5.19 Å. The first and second (turn) layer lines, being equally spaced about 1/10.5 $Å^{-1}$ apart, can be recognized clearly. Considering that the meridional reflection with the spacing of 1.5 Å (corresponding to the residue height of α-helix) is observed by using a cylindrical camera, the most probable form of the molecule may be an α-helical conformation with a 7/2 screw. The density calculated on this basis is 1.24 g/cm^3, which is in good agreement with the value (1.24 g/cm^3) directly observed by the flotation method.

Figures 5b−d illustrate the X-ray diffraction patterns taken at 140 °C (between T_1 and T_2), 150 °C (between T_2 and T_3), and 160 °C (above T_3). For such high-temperature forms, only the reflections with spacings larger than 3.5 Å were detected because of the limited size of the window of the hot stage. As indicated by a comparison of Figures 5a and 5b, the profiles of the diffraction patterns are improved above the T_1 transition: i.e., several sharp reflections can be observed on the layer lines as well as on the equatorial line. All of these reflections can be indexed by assuming a three-dimensional orthorhombic lattice with $a = 28.0$ Å, $b = 16.1$ Å, and $c = 10.5$ Å, which accommodates two PPPLA chains; the two-dimensional lattice obtained from the equatorial reflections still has a hexagonal symmetry (Table 2). At temperatures between the T_2 and T_3 transitions, the layer line reflections again become diffuse while the equatorial reflections still remain sharp (see Figure 5c). This may probably be caused by the activated rotational and translational motions of helical molecules.[19] Changes observed in the diffraction patterns at the T_1 and T_2 transitions are apparent, but the chain conformation (7/2 α-helical form) and the lateral packing of molecules (a hexagonal symmetry) are essentially retained at these transitions.

The significant change takes place at the T_3 transition. As manifestly shown in Figure 5d, the layer line profile changes drastically, where a single layer line is observed at a height of 1/4.93 $Å^{-1}$. Equatorial reflections can be interpreted as a lateral packing of molecules with a simple hexagonal symmetry but with an expanded intermolecular spacing (see Table 2). Figure 6 shows the variation of the spacing of the first equatorial reflection (d_{100}) with temperature. The value

Table 2. X-ray Diffraction Data of PPPLA at 30, 140, 150, and 160 °C

30 °C		140 °C				150 °C		160 °C	
d_{obs} (Å)[a]	$h'k'0$[b]	d_{obs} (Å)[a]	$h'k'0$[b]	hkl[c]	d_{calc}(Å)[c]	d_{obs}(Å)[a]	$h'k'0$[b]	d_{obs} (Å)[a]	$h'k'0$[b]
equatorial line		equatorial line				equatorial line		equatorial line	
13.40 vs	(100)	13.90 vs	(100)	(200)	13.98	14.00 s	(100)	15.20 vs	(100)
7.88 m	(110)	8.05 m	(110)	(310)	8.07	8.05 m	(110)	8.65 w	(110)
6.74 m	(200)	7.00 w	(200)	(400)	6.99	7.02 w	(200)	7.52 w	(200)
first layer line		first layer line				first layer line			
~5.5 (broad)		6.30 vvw		(311)	6.39	streak			
		5.10 m		(321)	5.27				
second (turn) layer line		second (turn) layer line				second (turn) layer line		turn layer line	
5.19 s		5.23 m		(102)	5.15	streak		4.93 vs	
~4.50 (broad)		4.77 vvw		(212)	4.70				
~4.00 (broad)		4.51 w		(312)	4.40				
		4.00 w		(322)	3.98				
		3.74 vvw		(512)	3.72				

[a] The data are collected from the X-ray photographs of Figure 5. At room temperature (30 °C), the reflections with spacings larger than 1.2 Å were detected by using a cylindrical camera, and the diffraction profile observed indicates that the molecules assume an α-helical (7/2) conformation with a repeat length of 1.5 Å (see text). For the high-temperature phases, only the reflections with spacings larger than 3.5 Å were observed because of the limited size of the window of the hot stage. [b] Based on a two-dimensional hexagonal lattice. [c] Based on an orthorhombic lattice with $a = 28.0$ Å, $b = 16.1$ Å, and $c = 10.5$ Å.

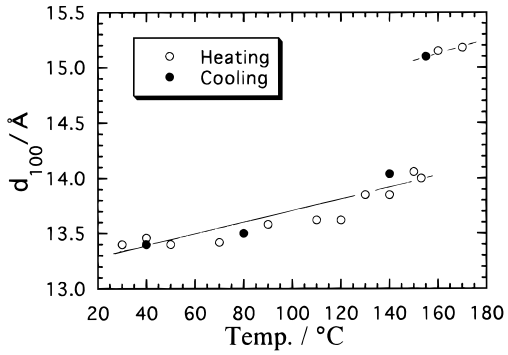

Figure 6. Temperature dependence of the spacing of the first equatorial reflection (d_{100} in the two-dimensional hexagonal lattice). The open and closed circles were collected on heating and cooling, respectively.

increases gradually with an increase in temperature until an abrupt jump takes place at T_3 (160 °C). The temperature dependence of the spacing shown in Figure 6 yields a thermal linear expansion coefficient of about 4×10^{-4}/K for the range between 30 and 160 °C, which is normal for this type of material.[19] The discontinuous lattice expansion observed at the T_3 transition is due to an increase in the diameter of helical molecule, or in other words, a reduction in the unit height (h) per residue along the helical backbone axis. Although the meridional reflection attributable to the unit height cannot be detected because of the difficulty in measurement, the value of h is calculated to be 1.27 Å by assuming that the density change is negligibly small at the T_3 transition. A similar small value of h (1.17 Å) has been reported for PPLA in the region above 130 °C; the skeletal conformation is suggested to be a π-helix, and the strong layer reflection at 4.93 Å observed here can be explained as a turn layer line.[11]

It is noteworthy that the changes in the gross dimensions of the oriented film at the T_3 transition were followed by optical microscopy. Figure 7 shows micrographs of a typical oriented film at 150 and 170 °C, where we see a striking decrease in length and an increase in width at the higher temperature. The length and width stay approximately constant before and after the T_3 transition, at which they change sharply. There can be seen a 13% decrease in the length, which compares with the increase of ∼5% in the width. This 13% reduction in length can also account for the change of the h value from 1.50 to 1.27 Å.

In order to get further information on the backbone conformation, ^{13}C CP/MAS TOSS NMR measurements were performed over a temperature range from 30 to 160 °C. Some representative spectra obtained at various temperatures are shown in Figure 8. The assignment of the chemical shifts has been adopted from the literature,[20−22] and the corresponding values observed are listed in Table 3. Among the chemical shifts listed, C(amide) and C$^{\alpha}$ arise from the carbon atoms tightly fixed to the backbone. The values observed are nearly constant at 175.4 and 54.3 ppm, respectively, over the temperature range from 30 to 150 °C, in agreement with those of the right-handed α-helical conformation of polypeptides. At 160 °C ($> T_3$), the chemical shifts C(amide) and C$^{\alpha}$ are reduced to 172.4 and 52.6 ppm, respectively. These values were found to fall in the range assigned to left-handed arrangements such as α-helix, ω-helix,[20,21] and π-helix[22] of PBLA and PPLA: for comparison, relevant values are also listed in Table 3. The most probable conformation of the high-temperature form would be a π-helix. As shown in the table, the variation of the chemical shifts (C$^{\beta}$, C(ester), C$^{\epsilon}$, and C^{ph}) due to the side-chain carbons is much smaller for the same transition.

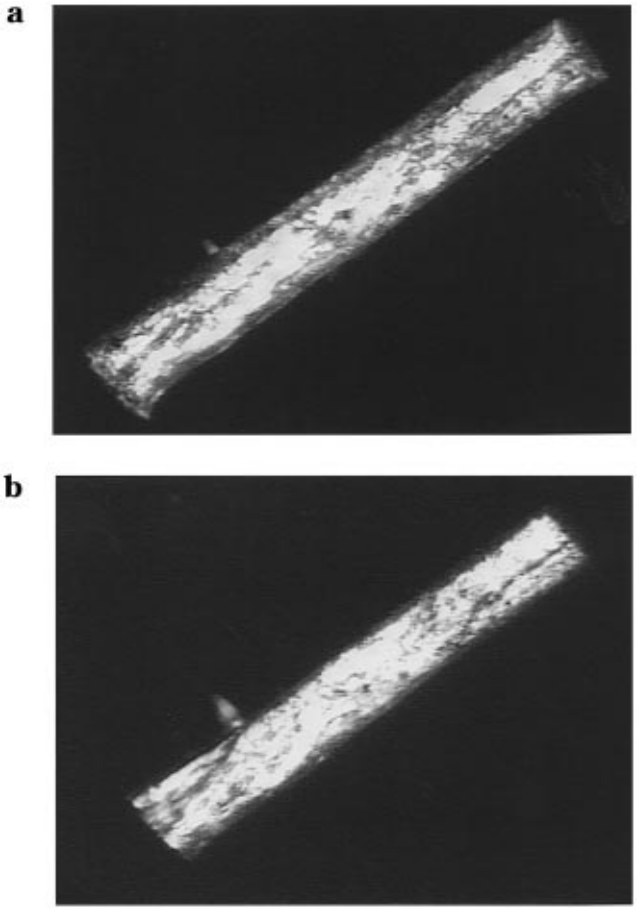

Figure 7. Optical micrographs of an oriented film of PPPLA at (a) 150 and (b) 170 °C.

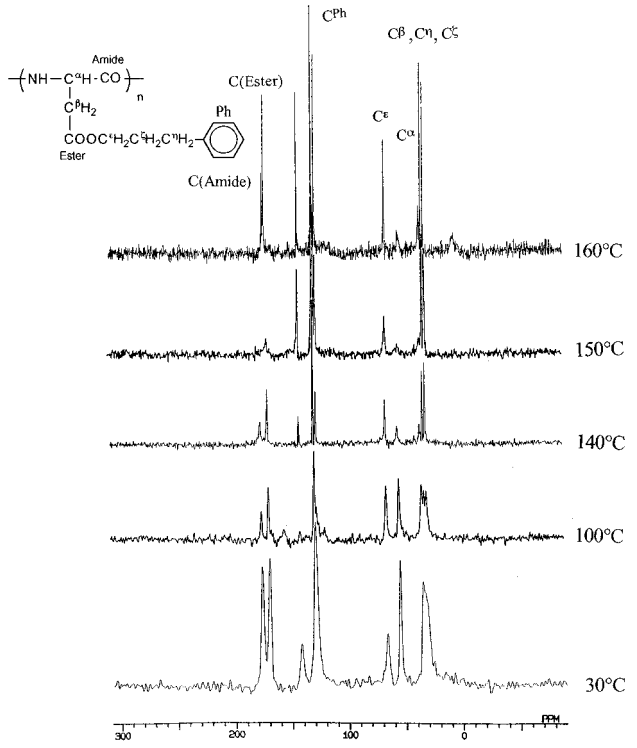

Figure 8. ^{13}C CP/MAS NMR spectra of PPPLA in the solid state at various temperatures.

Table 3. Temperature Dependence of ^{13}C Chemical Shifts for PPPLA in the Solid State and Reference Data for PPLA and PBLA

polymer	helix	temp (°C)	chem shifts (ppm) C^{α}	C(amide)	C^{β}	C(ester)	C^{ϵ}	C^{ph}	ref
PPPLA		30	54.3	175.4		169.1	65.3	128.8	
		100	54.3	175.2	34.5	169.2	65.2	128.8	
		140	54.6	175.3	34.1	170.0	65.1	130.0	this work
		150	54.4	174.9	34.6	170.0	65.1	130.1	
		160	52.6	172.4	34.4	170.9	64.6	130.0	
PPLA	$^{\alpha}$R	30	54.4	175.4		169.5			22
	$^{\pi}$L	150	52.3	172.4	33.9	171.2			22
PBLA	$^{\alpha}$R	23	54.4	175.9	34.8	168.0			20, 21
	$^{\alpha}$L	30	51.9	172.1	34.8	170.0			20, 21
	$^{\omega}$L	30	50.5	172.3	33.9	168.8			20, 21

4. Discussion

It has been concluded from a combined use of CD and X-ray measurements that a reversible helix−helix transition with screw-sense inversion takes place in the solid state as well as in dilute solution. The transition was found to be moderately sharp and reversible, indicating that it is of a first order. X-ray and CP/MAS NMR data suggest that a right-handed α-helix transforms to a left-handed helical form. An approximate value of the unit height estimated for the high-temperature form is 1.27 Å. This value is fairly smaller than that of the α-helix (1.5 Å) and reasonably close to the value proposed for the π-form by Low et al.[23,24] (1.15 Å) and by Sasaki et al.[11](1.17 Å).

In the π-helix, hydrogen-bonds are formed between the C═O of the *i*th residue and the N−H of the (*i* + 5)th residue, while in the α-helix, the *i*th C═O and (*i* + 4)th NH participate in a hydrogen-bond pair. An important observation is that the helix-sense inversion occurs at T_3 without disturbing the uniaxial ordering of helical molecules. This can be recognized from a comparison of the oriented X-ray patterns of Figures 5c and 5d. The birefringence measurements were also consistent with this scheme. Hence, the helix−helix transformation between the two opposite regimes should involve a mechanism in which an unwinding and rewinding of the helical screw takes place concertedly along the backbone.

Accumulation of various experimental evidences suggest that the side-chain conformation may play a key role in triggering such transitions. Examples are abundantly known for conventional polymers in which the conformational asymmetry involved in the side chain largely affects the spatial configuration of the skeletal chain.[25−28] In an asymmetric polymer, the side-chain conformation varies more or less with the configuration of the main chain. Since bond conformations are often neighbor dependent along the polymer chain, small free energy differences accumulated in the individual side chains may become a driving force for a large deformation of the skeletal chain.[8,10,22] Since helical polypeptides are regularly hydrogen bonded, the screw-sense inversion inevitably occurs in a highly cooperative fashion. Essentially the same mechanism has been presented for the thermally induced helix−helix inversion observed for a racemic mixture comprising PPLA and PPDA in the solid state.[29]

References and Notes

(1) Bradbury, E. M.; Downie, A. R.; Elliott, A.; Hanby, W. E. *Proc. R. Soc. London, Ser.* A **1960**, *259*, 110.
(2) Karlson, R. H.; Norland, K. S.; Fasman, G. D.; Blout, E. R. *J. Am. Chem. Soc.* **1960**, *82*, 2268.
(3) Goodman, M.; Boradman, F.; Litowsky, L. *J. Am. Chem. Soc.* **1963**, *85*, 2491.
(4) Hashimoto, M.; Arakawa, S. *Bull. Chem. Soc. Jpn.* **1967**, *40*, 1698.
(5) Bradbury, E. M.; Carpenter, B. G.; Goldman, H. *Biopolymers* **1968**, *6*, 837.
(6) Abe, A.; Okamoto, S.; Kimura, N.; Tamura, H.; Onigawara, H.; Watanabe, J. *Acta Polym.* **1993**, *44*, 54.
(7) Watanabe, J.; Okamoto, S.; Abe, A. *Liq. Cryst.* **1993**, *15*, 259.
(8) Okamoto, S.; Furuya, H.; Abe, A. *Polym. J.* **1995**, *27*, 746.
(9) Yamamoto, T.; Honma, R.; Nishio, K.; Hirotsu, S.; Okamoto, S.; Furuya, H.; Watanabe, J.; Abe, A. *J. Mol. Struct.* **1996**, 375, 1.
(10) Okamoto, S.; Furuya, H.; Abe, A. *Vysokomol. Soedin. (Polym. Sci.)*, in press.
(11) Sasaki, S.; Yasumoto, Y.; Uematsu, I. *Macromolecules* **1981**, *14*, 1797.
(12) Giancotti, V.; Quadrifoglio, F.; Crescenzi, V. *J. Am. Chem. Soc.* **1972**, *94*, 287.
(13) Kyotani, H.; Kanetsuna, H.; Oya, M. *J. Polym. Sci., Polym. Phys. Ed.* **1977**, *15*, 1029.
(14) Sasaki, S.; Ogawa, H.; Kimura, S. *Polym. J.* **1991**, *23*, 1325.
(15) Okabe, M.; Yamanobe, T.; Komoto, T.; Watanabe, J.; Ando, I. *J. Mol. Struct.* **1989**, *213*, 213.
(16) Daly, W. H.; Poche, D. *Tetrahedron Lett.* **1988**, *29*, 5859.
(17) Hayashi, Y.; Teramoto, A.; Kawahara, K.; Fujita, H. *Biopolymers* **1969**, *8*, 403.
(18) Dixon, W. T.; Shafer, J.; Sefcik, M. D.; Stejskal, E. O.; Mckay, R. A. *J. Magn. Reson.* **1982**, *49*, 341.
(19) Watanabe, J.; Naka, M.; Watanabe, J.; Watanabe, K.; Uematsu, I *Polym. J.* **1978**, *10*, 569.
(20) Saito, H.; Tabeta, R.; Ando, I.; Ozaki, T.; Shoji, A. *Chem. Lett.* **1983**, 1437.
(21) Tuzi, S.; Ando, I.; Shoji, A.; Ozaki, T. *J. Mol. Struct.* **1990**, *238*, 347.
(22) Okamoto, S. Ph.D. Thesis, Tokyo Institute of Technology, 1995.
(23) Low, B. W.; Baybutt, R. B. *J. Am. Chem. Soc.* **1952**, *74*, 5806.
(24) Low, B. W.; Grenville-Wells, H. J. *Proc. Natl. Acad. Sci. U. S. A.* **1953**, *39*, 785.
(25) Abe, A. Chain Conformation. In *Comprehensive Polymer Science*; Booth, C., Price, C., Eds.; Pergamon Press: Oxford, 1989; Vol. *2*, Chapter 2.
(26) Abe, A. *J. Am. Chem. Soc.* **1968**, *90*, 2205.
(27) Abe, A. *J. Am. Chem. Soc.* **1970**, *92*, 1136.
(28) Abe, A. *Macromolecules* **1977**, *10*, 34.
(29) Okamoto, S.; Furuya, H.; Watanabe, J.; Abe, A. *Polym. J.* **1996**, *28*, 41.

MA9605964